TRANSLAMINAR FRACTURE TOUGHNESS OF CFRP: FROM THE TOUGHNESS OF INDIVIDUAL PLIES TO THE TOUGHNESS OF THE LAMINATES.

R. F. Teixeira[1*], S. T. Pinho,[1] and P. Robinson[1]

[1]*Department of Aeronautics, Imperial College London, London, SW7 2AZ, UK*

[*]*rita.teixeira07@imperial.ac.uk*

Keywords: Translaminar fracture toughness, Ply orientation, Micrography, Compact Tension.

Abstract

The translaminar fracture toughness of carbon-epoxy multidirectional composite laminates was measured using a compact tension (CT) configuration. Additionally, translaminar fracture toughnesses of individual plies orientated at angles of $90°$, $0°$ and $\pm 45°$ were determined. The fracture surfaces of the CT specimens were analysed to investigate relationships between the features of these surfaces and the toughness measurements. Failure mechanisms found in the multidirectional laminates included a combination of the failure mechanisms found on bi-directional laminates $(90/\theta)$ made of its constituent plies. Ply splitting, fibre bridging and fibre pull were the main features characterizing the fracture surfaces. Three analytical predictive models were used to predict the translaminar toughness of the laminates from that of the constituent plies. The assumption of translaminar fracture toughness additivity by means of a law of mixtures correlated best with the experimental results.

1 Introduction

Failure mechanisms (such as fibre-matrix debonding, fibre fracture, fibre bridging/pull-out, matrix cracking, delamination) in composite materials have been intensively investigated since the 1920's and they are not yet fully understood [1]. Most of the work done on fracture toughness, measured for different laminates [2–6], focuses on initiation fracture toughness values. Some authors have measured the toughness of sublaminates with the objective of relating it to the toughness of a laminate using the rule of mixtures. Similarly, Pinho et al [7] and Laffan et al [8] used the rule of mixtures to calculate the toughness of $0°$ plies using cross-ply laminates. Indirectly, the analytical models by Poe [3] and Vaidya and Sun [5] also allow for the calculation of the $0°$ ply fracture toughness from the laminate's.

While the rule of mixtures assumes that the contribution of the energy dissipated by each ply in a laminate is additive, i.e., the failure processes in one ply do not affect the failure processes in another, the models by Poe [3] and Vaidya and Sun [5] assume that fracture of the laminate occurs upon fracture of the fibres in the load bearing plies (typically those plies aligned with the loading). There is currently little published data on experimental evidence fully supporting either approach. In particular, none are able to predict the size and ply blocking effects observed experimentally [9, 10].

This paper aims to investigate experimentally how translaminar toughness of a laminate relates to that of its plies (with different ply-block thicknesses and different ply orientations), by obtaining experimentally the resistance curves (R-curves) both for the plies and laminate from the. The fracture surfaces were examined using optical and SEM micrography to find relationships between the features of these surfaces and the experimental data.

2 Experimental method and data reduction

2.1 Material System

The material system used in this work was the unidirectional (UD) carbon-epoxy prepeg T800s/M21 provided by Hexcel. Table 1 presents the relevant material properties.

	Measured	
	Average	Std dev
Longitudinal Tensile Strength [MPa]	3067	157
Longitudinal modulus E_{11} [GPa]	160.4	5.3
Transverse Tensile Strength [MPa]	43.9	7.6
Transverse modulus E_{22} [GPa]	9.3	0.2
Poisson's Coefficient ν_{12}	0.33	0.02
Shear modulus G_{12} [GPa]	-	-

Tab. 1: T800s/M21 measured elastic properties.

2.2 Specimen and layup configuration

Compact Tension (CT) specimens with the dimensions and orientation shown in Figure 1 have been used.

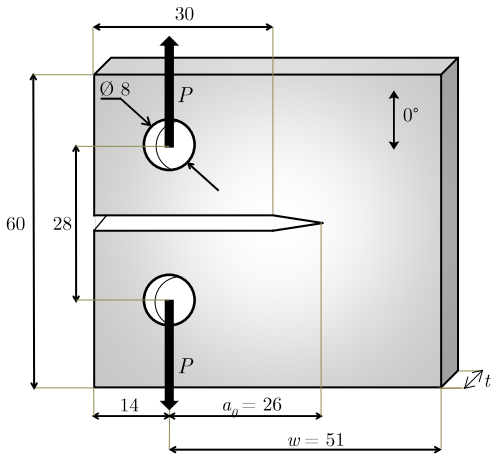

Fig. 1: CT specimen dimensions and fibre directions. All dimensions are in mm.

All layups were manufactured using hand layup and cured in an autoclave according to the manufacture recommendations. A wet saw was used to cut the rectangular plates into the specimen's geometry (Figure 1). Two 8 mm holes were drilled using a carbide tipped drill. A notch was machined using a diamond coated disk-saw to guarantee an accurate and sharp crack tip. With the objective of relating the fracture toughness if individual plies to that of different laminates, the layups detailed in Table 2 were manufactured.

Layup	Purpose of Layup
$[90_{34}]$	G_{Ic} of $[90]_{34}$
$[(90/0)_8/90]_s$	G_{Ic} of 0°
$[(90_6/0)_2/90_3]_s$	G_{Ic} of 0°
$[(90_5/0_2)_2/90_3]_s$	G_{Ic} of 0°_2
$[(90_6/-45)/(90_6/+45)/90_3]_s$	G_{Ic} of 45°
$[(90_5/-45)/+45/90_3]_s$	G_{Ic} of $\pm 45^\circ$
$[90_6/+45/0/-45/90_3]_s$	G_{Ic} of laminate
$[90/+45/0/-45]_{3s}$	G_{Ic} of laminate
$[90_2/0_2/+45_2/-45_2/90/0/+45/-45]_s$	G_{Ic} of laminate

Tab. 2: Investigated layups. 0° is aligned with the direction of the applied load

Six CT specimens for each layup as indicated in Table 2 were tested using an Instron machine with a 10 kN load cell. Each specimen was loaded with a constant displacement rate of 2 mm/min to obtain quasi-static conditions.

2.3 Data Reduction

2.3.1 Laminate fracture toughness

The data reduction for CT specimens was done using the *modified compliance calibration* method [8]. The compliance C calibration vs. crack length a curve is obtained by using FE and the critical energy release rate of the laminate G_{Ic}^{Lam} is determined by:

$$G_{Ic}^{\text{Lam}} = \frac{P_c^2}{2t}\frac{\mathrm{d}C}{\mathrm{d}a} \tag{1}$$

where P_c is the maximum measured load that initiates fracture and t the specimen's thickness. One of the main advantages of this data reduction method is that it does not rely on the observation of the surface of the specimen. The external plies of the specimen do not reflect the actual crack tip growth since the crack front is not necessarily uniform through the thickness and delamination near the crack relaxes the strain field.

2.3.2 Ply fracture toughness

Once the critical energy release rate for the laminate was obtained, the critical energy release rate for the ply of interest (see Table 2) was calculated by accounting for the toughness corresponding to matrix cracking in the 90° layers using superposition (Law of Mixtures). Following previous work [7, 8, 11], this procedure neglects other damage modes such as delamination, as well as any interaction between matrix cracking and the fibre dominated failure modes, and assumes that a single matrix crack parallel to the pre-crack occurs in the 90° layers. A through thickness mode I crack for a general orthotropic laminate can be related to the corresponding ply the law of mixtures expressed as:

$$G_{Ic}^{\text{Lam}} = \frac{\sum_{i=1}^{N} G_{Ici} t_i}{t_{\text{Lam}}} \tag{2}$$

where G_{Ic}^{Lam} represents the critical strain energy release rate for the laminate, G_{Ici} represents the critical strain energy release rate for each ply, t_{Lam} is the total laminate thickness and t_i is the total thickness for all plies oriented at an angle i.

3 Results

All the specimens exhibited a clear R-curve effect, as observed for representative specimens in Figure 2 where the first point corresponds to the first significant load-drop. For each specimen, an initiation value can be defined as the first toughness measurement, while the propagation values are slightly more subjective and were simply defined as the values for which the R-curves appeared to converge at. The average critical energy release rates obtained for initiation and propagation are listed in Table 3.

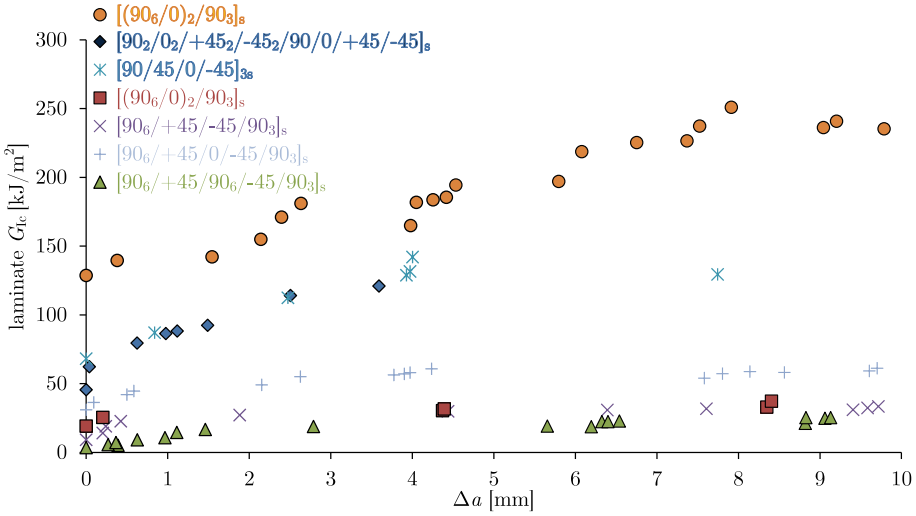

Fig. 2: R-curves for laminate-level translaminar fracture toughness.

Laminate	**Ply**	G_{Ic}^{ply} [kJ/m^2] (CoV %) **Initiation**	G_{Ic}^{ply} [kJ/m^2] (CoV %) **Propagation**
$[(90/0)_8/90]_s$	0°	151(19.8)	269(13.6)
$[(90_6/0)_2/90_3]_s$	0°	205(7.8)	283(7.4)
$[90_5/0_2/90_3]_s$	0_2°	400(11.3)	653(22.4)
$[(90_6/-45)/(90_6/+45)/90_3]_s$	45°	40(21.7)	191(8.3)
$[90_6/-45/+45/90_3]_s$	-	55(18)	167(11)
Laminate	**-**	G_{Ic}^{Lam} [kJ/m^2] (CoV %) **Initiation**	G_{Ic}^{Lam} [kJ/m^2] (CoV %) **Propagation**
$[(90/0)_8/90]_s$	–	112.13(3.75)	129.52(8.63)
$[(90_6/0)_2/90_3]_s$	–	19.34(14.5)	30.30(12.9)
$[90_5/0_2/90_3]_s$	–	94.11(11.3)	155.3(24.9)
$[(90_6/-45)/(90_6/+45)/90_3]_s$	–	4.61(34)	22.57(8.9)
$[90_6/-45/+45/90_3]_s$	-	10.4(15.9)	30.80(10.1)
$[90_6/+45/0/-45/90_3]_s$	-	34(87)	62(7.0)
$[90/+45/0/-45]_{3S}$	-	77(13.4)	150(8.0)
$[90_2/0_2/+45_2/-45_2/90/0/+45/-45]_s$	-	63(22.5)	$> 118(-)$

Tab. 3: Average initiation and propagation values of critical energy release rates for each laminate investigated.

Post-mortem analyses, using Scanning Electron and Optical Microscopy, were used to investigate the different damage modes as well as their sequence of occurrence. Typical images

of the fractured surfaces are shown in Figures 3-4.

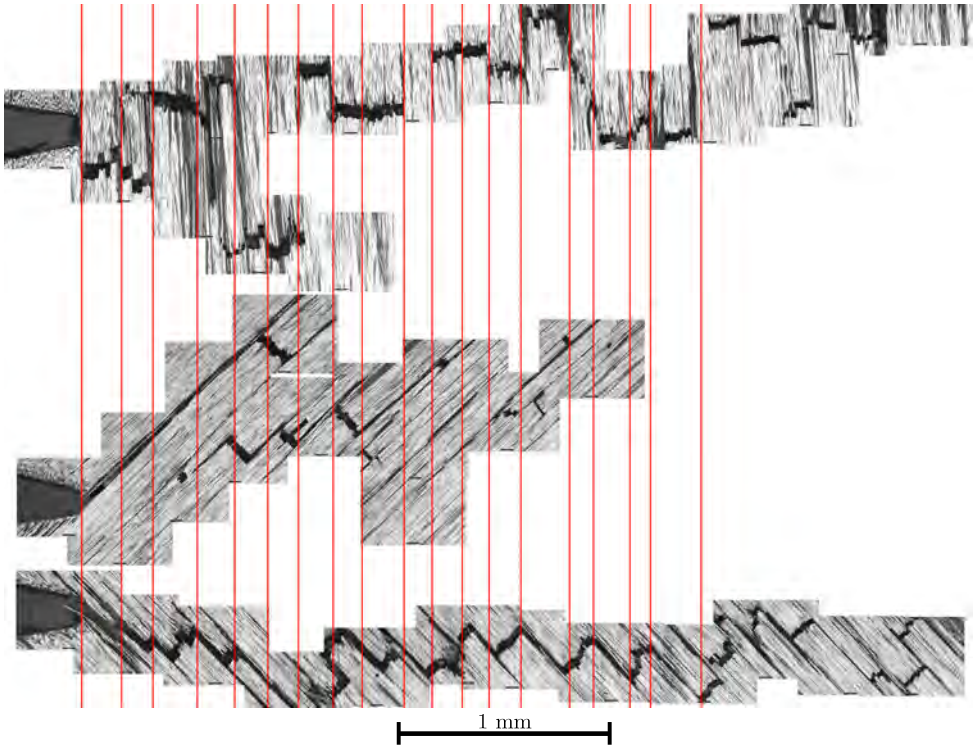

Fig. 3: Micrographs of a $[90_6/+45/0/-45/90_3]_s$ specimen. Top: $0°$ ply. Middle: $+45°$ ply. Bottom: $-45°$ ply.

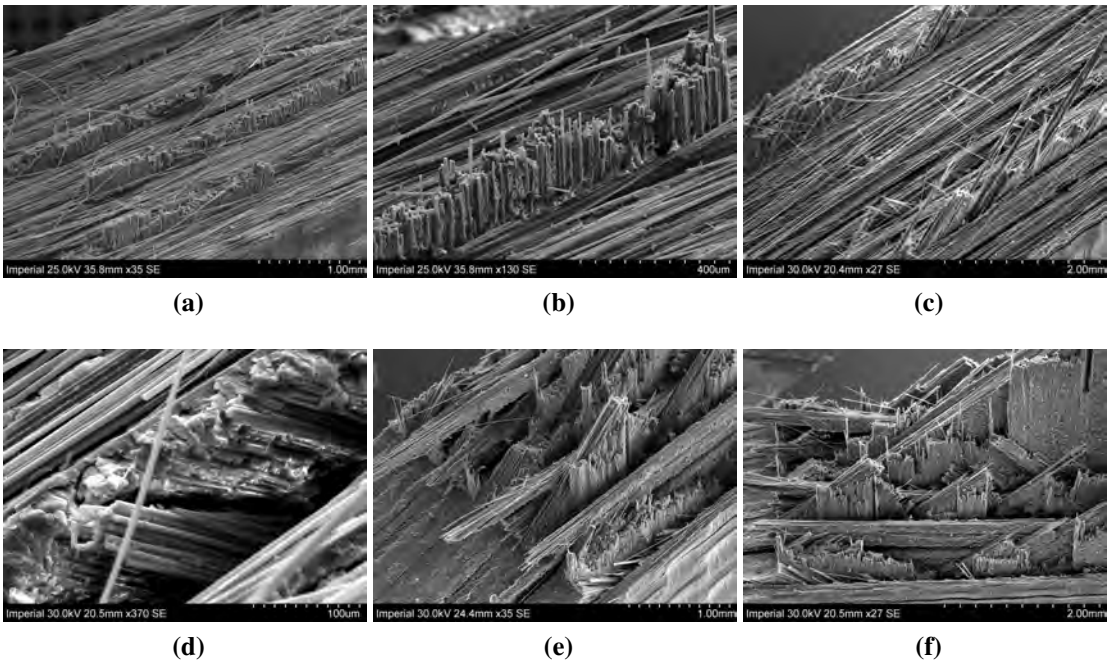

Fig. 4: (a) Fracture surface of the $[(90_6/0)_2/90_3]_s$ laminate. (b) Magnification of a bundle of fibres pull-out in the same specimen. (c) Fracture surface of a $[(90_6/-45)/(90_6/+45)/90_3]_s$ laminate (c). (d) Delamination in the $45°/90°$ interface of laminate . (e) Crack tip of a $[90/+45/0/-45]_{3s}$ specimen. (f) Saw-tooth like pull-out.

4 Discussion

4.1 Experimental results

A stick-slip crack typically between 2 and 2.5 mm was found in all CT specimens during testing. Upon reaching the critical load, fracture propagated consistently and stably (high number of crack jumps) and arrested at some lower value of load.

All specimens exhibited a clear R-Curve effect as observed previously in Figure 2. Propagation values were in general less scattered (lower CoV) than initiation values (Table 3). This can be explained by the fact that propagation values depend on the development and interaction of complex failure mechanisms over crack growth (and therefore some averaging takes place), while initiation stems from the first failure of the fibres at a well defined notch which is only one event per specimen. The R-Curves obtained from $[(90/0)_8/90]_s$ and $[(90_6/0)_2/90_3]_s$ specimens demonstrated that the 0° ply toughness was not found to increase significantly when increasing the number of 0° plies from 4 to 16 (Table 3). For the blocked 0° plies' laminates (Figures 2), the process zone is significantly longer than in the no blocked 0° plies case (Figure 2), which is translated into a significant toughness increase that occur before *steady state* can be reached. The propagation toughness of the blocked 0° plies is almost three times greater than in the case of its baseline configuration (Table 3).

Under the SEM, both $[(90_6/0)_2/90_3]_s$ and $[(90_6/-45)/(90_6/+45)/90_3]_s$ fracture surfaces exhibited flat regions of the 90° fibres and blocks of fibres pulled-out. The latter consisted mainly of bundles rather than single fibres (Figures 4a-4c). In $[(90_6/-45)/(90_6/+45)/90_3]_s$ specimens, the first event is the occurrence of ply splitting along the 90° layers. This caused delamination between the 90° plies and their adjacent layers and induced splitting in the $\pm 45^\circ$ plies, causing further delamination in these plies (Figure 4d). $\pm 45^\circ$ plies failed under in-plane-shear, developing a saw-tooth appearance. From Figures 4e and 4f, it can be seen that 0° plies failed through steps (also highlighted in Figures 4a and 4b) while $\pm 45^\circ$ failed in a saw-tooth like manner (Figure 3). $\pm 45^\circ$ and 0° plies appeared to fail independently because of the distinctive crack paths found in adjacent plies in $[90_6/+45/0/-45/90_3]_s$ specimens (Figure 3). An interesting phenomena can be noticed in Figure 3 where fibre bundles in the $\pm 45^\circ$ and 0° plies appear to fail coordinately, though following different paths, with an approximately similar length in between failed bundles. Each load drop was preceded by the failure of the load bearing plies: $\pm 45^\circ$ plies for laminates containing only $\pm 45^\circ$ & 90° plies and 0° plies for any other laminate (cross-ply or multidirectional).

The fibre pull-out length for the *steady state* phase, (i.e. once the translaminar fracture toughness has reached its propagation value) was measured in two specimens of each layup. Considerable scatter was noticed regarding pull-out height measurements which can be explained by the fact that the pull-out length is significantly higher in the midthickness plies (Figures 4e and 4f). Also, fibre pull-out on the 0° plies was conditioned by the 45° plies. When the $[-45^\circ/0^\circ/45^\circ]$ sub-laminate was isolated, as it was the purpose for the $[90_6/+45/0/-45/90_3]_s$ configuration, this idea was reinforced as the same effect was observed as in the quasi-isotropic laminates. The crack appeared to propagate through splits in the 45° plies and when the loading bearing 0° plies failed, the 45° plies broke and the crack propagated normal to the latter until it reached the initial crack plane. This loop carried on until final separation of the surfaces occurs.

Figures 3 and 4f corroborates the suggested sequence of events.

4.2 Analytical results - Translaminar fracture toughness predictions

Three analytical models were used to calculate the translaminar fracture toughness of the laminates:

- Rule of Mixtures (Equation (2))
- Poe's model [3]
- Vaidya and Sun's model [5]

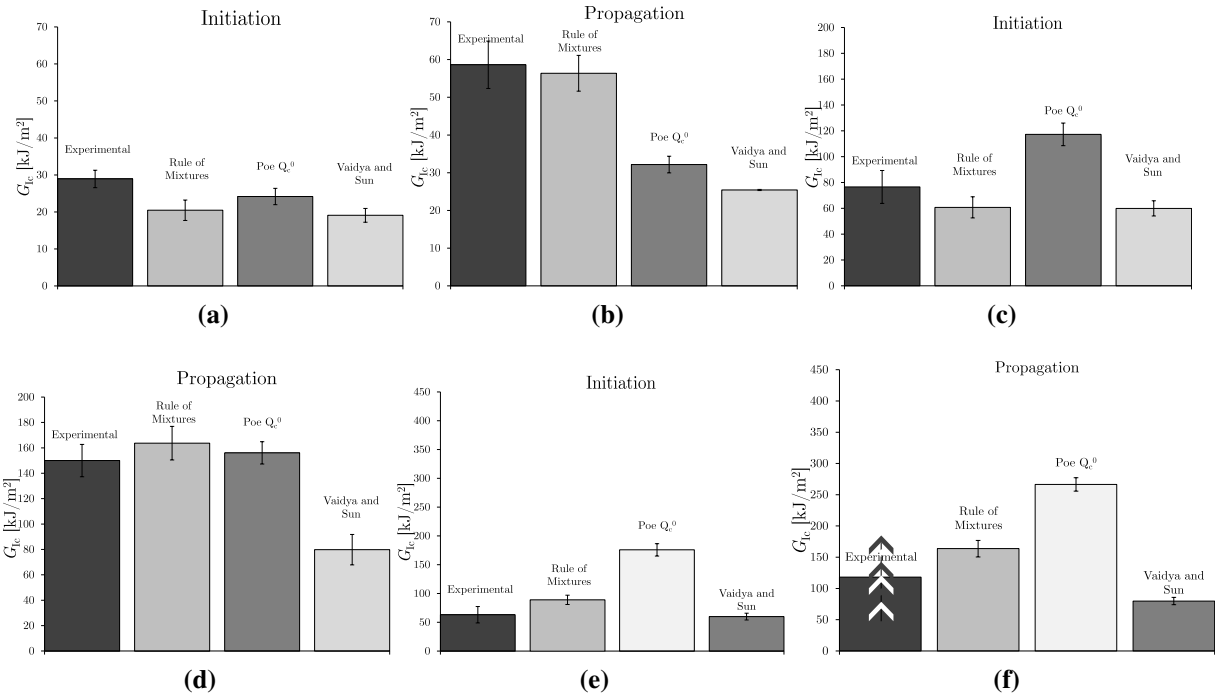

Fig. 5: (a) Initiation toughnesses for $[90_6/+45/0/-45/90_3]_s$ specimens. (b) Propagation toughnesses for $[90_6/+45/0/-45/90_3]_s$ specimens. (c) Initiation toughnesses for $[90/+45/0/-45]_{3s}$ specimens. (d) Propagation toughnesses for $[90/+45/0/-45]_{3s}$ specimens. (e) Initiation toughnesses for $[90_2/0_2/+45_2/-45_2/90/0/+45/-45]_s$ specimens. (f) Propagation toughnesses for $[90_2/0_2/+45_2/-45_2/90/0/+45/-45]_s$ specimens.

Figure 5 shows that the rule of mixtures was the most consistent and accurate model in predicting the translaminar fracture toughness of the three multidirectional laminates. Considering the experimental variability (error bars in Figure 5), the prediction given by the rule of mixtures can be considered to agree particularly well. The small difference is likely to be due to fact that some failure mechanisms in quasi-isotropic laminates do not occur for the other configurations that only involve two different angle ply constituents. Poe's model overpredicted toughness values in both quasi-isotropic configurations. Vaidya and Sun's model correlated acceptably well with the experimental data, regarding initiation values. It gave conservative results in both initiation and propagation. It should be noted that propagation values in both Poe and Vaidya and Sun's models were not necessarily expected to correlate well due to the fact that both models use classical lamination theory and the damage that occurs near the crack plane during crack growth will therefore introduce a source of errors.

5 Conclusions

This study presents the experimental measurement of the translaminar fracture toughness, using the carbon-epoxy system T800s/M21, for 90°, 0° and $\pm 45^\circ$ plies. The material showed high fracture toughness values which can be explained by the high amount of pull-out of bundles of fibre verified from the analysis of the fracture surfaces using SEM. The effect of blocking two 0° plies together tripled the translaminar fracture toughness value whereas blocking 45° plies affected slightly the latter. The sequence of failure mechanisms was identified for each laminate through the inspection of the fracture surfaces by means of SEM and Optical microscopy.

The translaminar fracture toughness (both during initiation and propagation) of individual plies was successfully measured and used to calculate the translaminar fracture toughness of three multidirectional laminates. From three predictive analytical models considered, the Rule of Mixtures correlated best and more consistently with regards to the experimental data.

Acknowledgments

The funding provided by Airbus and FCT (Fundação para a Ciência e a Tecnologia) to make this research possible and participation in this conference is gratefully acknowledged.

References

[1] P. W. Beaumont, "The failure of composites: an overview," *Journal of strain analysis*, vol. 24, pp. 189–205, 1989.

[2] K. M. Prewo, "The effect of ply lay-up sequence on the fracture toughness of boron aluminum," *Journal of Composite Materials*, vol. 12, pp. 40–52, 1978.

[3] C. C. Poe, "A unifying strain criterion for fracture of fibrous composite laminates," *Engineering Fracture Mechanics*, vol. 17, pp. 153–171, 1983.

[4] C. E. Harris and D. H. Morris, "A comparison of the fracture behaviour of thick laminated composites utilizing compact tension, three-point bend and centre-cracked tension specimens," Tech. Rep. ASTM STP 905, Fracture Mechanics: seventh volume, 1986.

[5] R. S. Vaidya and C. T. Sun, "Fracture criterion for notched thin composite laminates," *AIAA Journal*, vol. 35, pp. 311–316, 1997.

[6] P. N. Dileep and R. Kumar, "A simple method for the evaluation of fracture toughness of a multi-layered laminate based on the failure stress of sub-laminates," *International Journal of Fracture*, vol. 131, pp. 3–6, 2005.

[7] S. T. Pinho, P. Robinson, and L. Iannucci, "Fracture toughness of the tensile and compressive fibre failure modes in laminated composites," *Composites Science and Technology*, vol. 66, pp. 2069–2079, 2006.

[8] M. J. Laffan, S. T. Pinho, P. Robinson, and L. Iannucci, "Measurement of the in situ ply fracture toughness associated with mode I fibre tensile failure in FRP. Part I:Data Reduction," *Composites Science and Technology*, vol. 70(4), pp. 606–613, 2010.

[9] M. J. Laffan, S. T. Pinho, P. Robinson, and L. Iannucci, "Measurement of the in situ ply fracture toughness associated with mode I fibre tensile failure in FRP. Part II:Size and lay-up effects," *Composites Science and Technology*, vol. 70(4), pp. 614–621, 2010.

[10] M. R. Wisnom, S. R. Hallett, and C. Soutis, "Scaling effects in notched composites," *Journal of Composite Materials*, vol. 44, pp. 195–210, 2010.

[11] T. A. Cruse, "Tensile Strength of Notched Composites," *Journal of Composite Materials*, vol. 7, p. 218, 1973.